Appl. Phys. A 69, 305–308 (1999) / Digital Object Identifier (DOI) 10.1007/s003399900121

Applied Physics A
Materials
Science & Processing

Synthesis, integration, and electrical properties of individual single-walled carbon nanotubes

J. Kong[1], C. Zhou[1], A. Morpurgo[2], H.T. Soh[3], C.F. Quate[3], C. Marcus[2], H. Dai[1]

[1] Department of Chemistry, Stanford University, Stanford, CA 94305, USA
(Fax: +1-650/725-0259, E-mail: hdai@chem.stanford.edu)
[2] Department of Physics, Stanford University, Stanford, CA 94305, USA
[3] E.L. Ginzton Laboratory, Stanford University, Stanford, CA 94305, USA

Received: 17 May 1999/Accepted: 18 May 1999/Published online: 14 July 1999

Abstract. High-quality single-walled carbon nanotubes (SWNTs) are synthesized by chemical vapor deposition (CVD) of methane on silicon-dioxide substrates at controlled locations using patterned catalytic islands. With the synthesized nanotube chips, microfabrication techniques are used to reliably contact individual SWNTs and obtain low contact resistance. The combined chemical synthesis and microfabrication approaches enable systematic characterization of electron transport properties of a large number of individual SWNTs. Results of electrical properties of representative semiconducting and metallic SWNTs are presented. The lowest two-terminal resistance for individual metallic SWNTs ($\approx 5\,\mu$m long) is $\approx 16.5\,k\Omega$ measured at 4.2 K.

PACS: 72.80.Rj; 73.61.Wp; 81.05.Tp; 81.15.Gh

Carbon nanotubes are atomically well-defined quasi one-dimensional systems that exhibit unique electrical, mechanical, and chemical properties. Single-walled nanotubes are ideal suited for studying low dimensional physics including band structures [1–7], electron-electron interactions [8], electron-lattice coupling [9, 10], and electron localization [10, 11]. Nanotubes are also promising candidates for nanometer-scale electronic devices. For instance, metallic–semiconducting junctions within single-walled nanotubes (SWNTs) may lead to transistors and Schottky rectifiers within a single nanotube molecule [12, 13].

While there has been considerable progress in understanding the electrical properties of nanotubes, as well as exploring their possible applications [14–16], what has been lacking is an efficient strategy for integrating nanotubes into electronic structures. In particular, it would be desirable from both a scientific and technological point of view to control not only the diameter and chirality of a SWNT, but also its length, position, and orientation. It is equally desirable to develop a means of making robust, low-resistance electrical contacts between nanotubes and metallic electrodes. These goals pose challenges to nanotube synthesis, processing, and assembly strategies.

Recently, we developed a chemical vapor deposition (CVD) method to synthesize high quality SWNTs on catalytically patterned surfaces [17]. This technique readily yields large numbers of SWNTs at specified locations, and opens up new possibilities in addressing the issues raised above. This paper describes the combination of this synthesis method with microfabrication techniques to obtain many nanotube-based electrical circuits on a single substrate with controllable positions and length (ranging from 300 nm to 10 μm), and to connect the tubes to macroscopic electrodes. We find that the contacts formed in this way often have very low resistance, of order of the quantum of resistance (tens of kilohms) even at low temperatures.

1 Synthesis of individual single-walled nanotubes on catalytically patterned surfaces

The synthesis procedure involves methane CVD on SiO_2 substrates that contain patterned catalyst islands. First, polymethylmethacrylate (PMMA) resist is spun onto a substrate. Electron-beam lithography is used to expose the PMMA film followed by developing the exposed resist to obtain an array of square wells in the PMMA film. The catalyst material consists of 15 mg of alumina nanoparticles, 0.05 mmol $Fe(NO_3)_3 \cdot 9H_2O$, and 0.015 mmol of $Mo_2(acac)_2$ in 15 ml of methanol. The mixture is stirred for 24 h and sonicated for 1 h before being deposited onto the substrate containing the patterned PMMA film. After solvent evaporation, the PMMA film is lifted off to obtain an array of catalyst islands on the substrate. CVD synthesis is carried out for 10 min at 900 °C in a 1-inch-diameter tube furnace using a methane flow rate of 5000 sccm/min. Under these conditions, nanotubes grown from the catalyst islands are predominantly individual SWNTs with few structural defects [17, 18]. The diameter distribution of the SWNTs is in the range of 0.7–5 nm with a peak at 1.5 nm [18]. As shown in Fig. 1, the synthe-

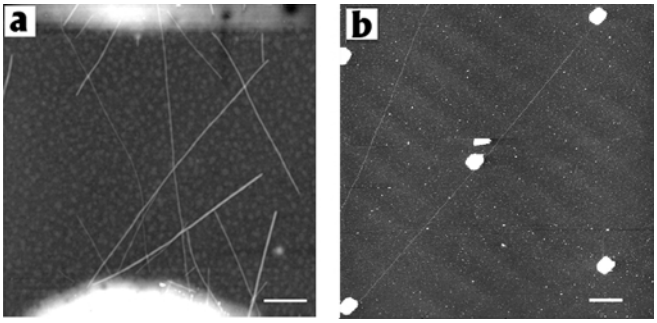

Fig. 1. a AFM image showing SWNTs grown off catalyst islands. The bright regions on the lower and upper part of the image are edges of two catalyst islands (size of islands $\approx 5\,\mu$m). Scale bar: 0.5 μm. **b** AFM image of an individual SWNT emanating and extending from the catalyst islands (bright spots, size of islands $\approx 1\,\mu$m). Scale bar: 2 μm

sized nanotubes emanate from the catalyst islands and are often found forming bridges between adjacent islands. SWNT bridging two islands are frequently observed [17]. A nanotube bridge forms when a tube growing from one catalyst island falls on and interacts with another island during the CVD process.

2 Integrating individual single-walled nanotubes into electrical circuits

After the CVD synthesis of a single-walled nanotube chip, electrical contact pads are placed over the catalyst islands (15 nm of Ti followed by 60 nm of Au) by electron-beam lithography and metal evaporation [19]. This step utilizes predefined alignment marks so that the metal contacts fully cover the catalyst islands and extended over their edges by 0.5 μm (Fig. 2a). Thus, the bridging SWNTs are contacted by the Ti metal film at both ends and sides. Optical and atomic force microscope (AFM) images of the SWNT circuits are shown in Fig. 2. As shown previously, the interactions between tube-island and tube-substrate are mechanically strong [17], allowing the nanotubes to withstand mechanical forces in the lithographic step for metal contacts. By setting the separation between the catalytic islands and varying the spacing between the edges of the metal pads, we are able to control the length of the nanotubes used for transport measurements. The lengths of the individual SWNTs that we have measured were in the range of 0.3–10 μm. Figure 2b shows a single SWNT connecting two metal pads spaced at $\approx 5\,\mu$m. When the pads are closely spaced ($< 1\,\mu$m), multiple tubes tend to bridge the gap. Using an AFM tip, we are able to cut nanotubes mechanically or electrically until a single tube is selected for electrical measurements.

Circuits formed by nanotube bridges between metal electrodes are first characterized at room temperature by measuring electrical resistance (with a 10 mV voltage bias) using a probe station (Signatone, model S-1160). Resistances ranging from 15 kΩ to several MΩ are normally observed. We find that the lower resistance tubes tend to remain good conductors at low temperatures. After this initial probing, an AFM is used to image the circuits of interest. We have concentrated our transport measurements on individual SWNTs with diameters in the range of 0.7–1.6 nm as revealed by the AFM apparent height data.

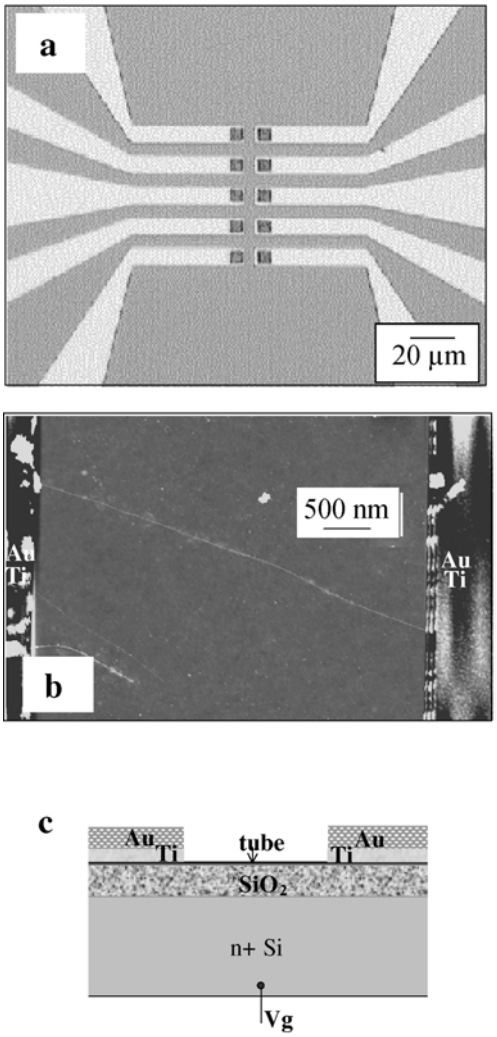

Fig. 2. a Optical micrograph of a set of devices containing 5 pairs of islands (*dark squares*) with electrodes (*light regions*). **b** AFM image of a SWNT bridging two metal pads in a finished device. **c** A schematic diagram showing the structure of the single-tube circuit

3 Results of transport measurements of individual SWNTs

Figure 3 shows the transport results obtained with several representative individual SWNTs bridging metal electrodes spaced at $\approx 5\,\mu$m. The current vs. voltage ($I-V$) curves for the semiconducting SWNT in Fig. 3a were taken at room temperature at different back-gate voltages. At zero gate voltage (V_g), the I–V curve appears to be approximately linear, indicating sufficient carrier density in the nanotube. The nanotube exhibits a linear resistance of $\approx 250\,$kΩ at room temperature and can carry current densities on the order of $\approx 10^8\,$A/cm^2 without breakdown. A strong non-linearity in I–V developed when the gate electrode was biased to a positive voltage with respect to the tube. Increasing V_g resulted in a complete suppression of the linear conductance. We observed a 6 orders of magnitude suppression of the linear conductance at $V_g \geq +6\,$V. Negative gate voltages slightly increased the conductance of the nanotube but saturated at $V_g \approx -2\,$V. These results are consistent with the obser-

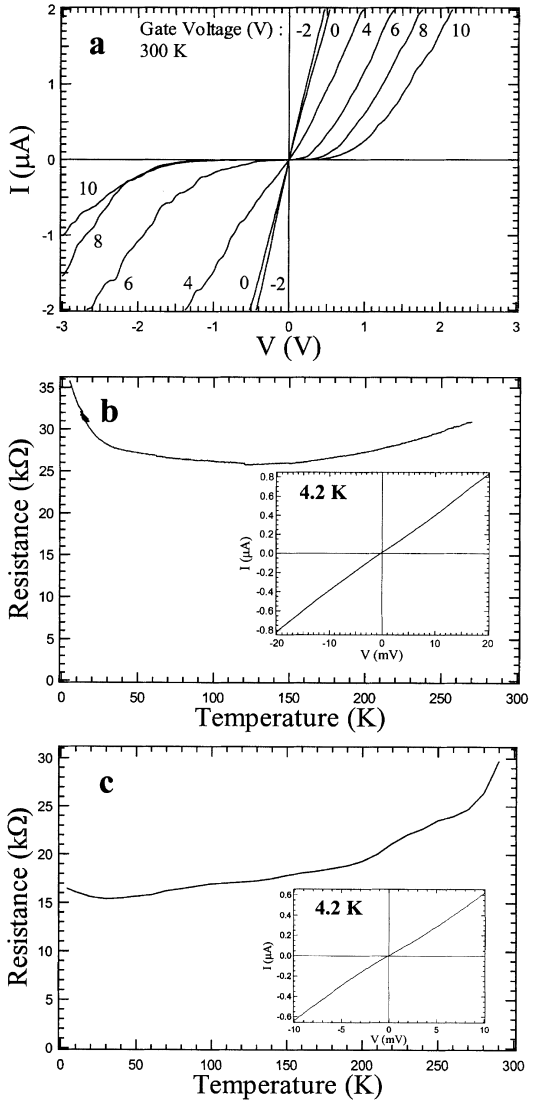

Fig. 3a–c. Electrical properties of three representative SWNTs. **a** *I–V* curves of a semiconducting SWNT for different values of gate voltage (V_g) measured at room temperature. **b** Resistance as a function of temperature for another SWNT. The *inset* shows an *I–V* curve taken at 4.2 K. The two-terminal resistance of this nanotube is $\approx 35\,\mathrm{k}\Omega$ at 4.2 K. **c** Resistance as a function of temperature for the third SWNT believed to be a true metallic arm-chair tube. The *inset* shows an *I–V* curve taken at 4.2 K. The two-terminal resistance of this nanotube is $\approx 16.5\,\mathrm{k}\Omega$ at 4.2 K

vations of room-temperature field-effect-transistor behavior of semiconducting nanotubes reported previously [16, 20]. Qualitatively, positive gate voltages cause the valence band to bend (down) away from the Fermi level, and thus lead to a reduction in the hole density in the semiconducting nanotube.

Significantly, our approach of nanotube synthesis combined with microfabrication techniques led to a large number of low-resistance SWNT devices. We often observed individual SWNTs exhibiting two-probe resistance less than $100\,\mathrm{k}\Omega$. Figure 3b shows the resistance vs. temperature curve of a SWNT that exhibits two-probe resistance of $\approx 30\,\mathrm{k}\Omega$ at room temperature and $\approx 35\,\mathrm{k}\Omega$ at 4.2 K. The resistance depends only weakly on temperature, showing an slight upturn at $T \approx 120\,\mathrm{K}$ and a more pronounced upturn upon further lowering the temperature below 30 K. This weak temperature dependence is generally regarded by previous studies as the signature of metallic SWNTs [10]. At 4.2 K, the *I–V* curve (inset) is essentially linear. When measured with a lock-in technique, the differential conductance showed a small increase in resistance at low bias. We did not observe Coulomb blockade oscillations with this nanotube at the lowest temperature reached in our experiment (1.7 K).

Figure 3c shows the result of resistance vs. temperature for a third SWNT. The resistance of this nanotube slowly decreases as the temperature decreases from 300 K, exhibits a slight upturn near $\approx 10\,\mathrm{K}$ but no pronounced increase in resistance upon further cooling down to 2 K, which differs from the behavior of the SWNT shown in Fig. 3b. At 4.2 K, the resistance was $\approx 16.5\,\mathrm{k}\Omega$ which is the lowest compared to the results obtained by previous experiments with individual single-walled tubes or ropes. The *I–V* curve (inset) recorded at 4.2 K is linear and no Coulomb blockade was observed down to $\approx 1.5\,\mathrm{K}$) in the experiment. These results suggest that the SWNT is an arm-chair nanotube that exhibits true metallic characteristics.

4 Summary

This work presents a chemical vapor deposition synthetic approach to high-quality single-walled carbon nanotubes. By patterning substrates with regular arrays of catalyst islands, we grow individual SWNTs at well-defined locations on surfaces, which allows controlled integration of nanotubes into electrical architectures by combining microfabrication techniques. The approach represents a new chemical route to novel nanotube materials that can be readily addressed individually. It is further demonstrated that our synthetic approach opens up new windows in systematically studying the physics in one-dimensional systems and exploring molecularly scale electrical devices at a large scale.

We have presented the results of electron transport studies of several representative SWNTs. The resistance of individual SWNTs were found to be ≈ 100 times smaller than that reported previously [14, 15]. It is plausible that a good electrical contact is established between the metal pads and the ends of the nanotubes. In particular, at the end where the nanotube originates from, chemical bonds between nanotube and the metal catalyst particle should be accounted for the excellent electrical contact [17]. At the present time, a complete understanding of the precise nature of the contacts is still being pursued. Future work in nanotube synthesis will focus on controlling the orientation of the SWNTs and the diameter and length of the nanotubes. Transport studies will focus on elucidating the intrinsic properties of various nanotubes as well as the nature of metal-tube contacts.

Acknowledgements. This work was supported by the National Science Foundation Partnership for Nanotechnology program (ECS-9871947), Stanford Center for Materials Research (a NSF-MRSEC), National Nanofabrication Users Network (funded by National Science Foundation ECS-9731294), the Camile Henry-Dreyfus Foundation, American Chemical Society DARPA/ETO, and National Science Foundation PECASE program (DMR-9629180-1).

References

1. M.S. Dresselhaus, G. Dresselhaus, P.C. Eklund: *Science of Fullerenes and Carbon Nanotubes* (Academic Press, San Diego 1996)
2. T.W. Ebbesen: Phys. Today **49**, 26 (1996)
3. R. Saito, M. Fujita, G. Dresselhaus, M.S. Dresselhaus: Appl. Phys. Lett. **60**, 2204 (1992)
4. N. Hamada, S.-i. Sawada, A. Oshiyama: Phys. Rev. Lett. **68**, 1579 (1992)
5. J.W. Mintmire, B.I. Dunlap, C.T. White: Phys. Rev. Lett. **68**, 631 (1992)
6. T. Odom, J. Huang, P. Kim, C.M. Lieber: Nature **391**, 62 (1998)
7. J.W.G. Wildoer, L.C. Venema, A.G. Rinzler, R.E. Smalley, C. Dekker: Nature **391**, 59 (1997)
8. C. Kane, L. Balents, M.P.A. Fisher: Phys. Rev. Lett. **79**, 5086 (1997)
9. C.L. Kane, E.J. Mele: Phys. Rev. Lett. **78**, 1932 (1997)
10. C.L. Kane, E.J. Mele, R. Lee, J.E. Fischer, P. Petit, H. Dai, A. Thess, R.E. Smalley, A.R.M. Verschueren, S.J. Tans, C. Dekker: Europhys. Lett. **6**, 683 (1998)
11. C.T. White, T.N. Todorov: Nature **393**, 240 (1998)
12. L. Chico, V.H. Crespi, L.X. Benedict, S.G. Louie, M.L. Cohen: Phys. Rev. Lett. **76**, 971 (1996)
13. P.G. Collins, A. Zettl, H. Bando, A. Thess, R.E. Smalley: Science **278**, 100 (1997)
14. S.J. Tans, M.H. Devoret, H. Dai, A. Thess, R.E. Smalley, L.J. Geerligs, C. Dekker: Nature **386**, 474 (1997)
15. M. Bockrath, D.H. Cobden, P.L. McEuen, N.G. Chopra, A. Zettl, A. Thess, R.E. Smalley: Science **275**, 1922 (1997)
16. S. Tans, A. Verschueren, C. Dekker: Nature **393**, 49 (1998)
17. J. Kong, H. Soh, A. Cassell, C.F. Quate, H. Dai: Nature **395**, 878 (1998)
18. J. Kong, A.M. Cassell, H. Dai: Chem. Phys. Lett. **292**, 567 (1998)
19. H. Soh, A. Morpurgo, J. Kong, C. Marcus, C. Quate, H. Dai: Appl. Phys. Lett. (1999), in press
20. R. Martel, T. Schmidt, H.R. Shea, T. Hertel, P. Avouris: Appl. Phys. Lett. **73**, 2447 (1998)